4

OPTICAL PROPERTIES OF CHROMIUM TRIHALIDES IN THE REGION 1-11 eV

P. M. Grant
G. Bryan Street

IBM Research Laboratory
San Jose, California 95114

The normal incidence optical reflectivity of thin single crystal platelets of $CrBr_3$ and CrI_3 has been measured over the range 1-11 eV. $CrBr_3$ is hexagonal with the c-axis normal to the platelet surface; CrI_3 is believed to have the same structure. Each Cr^{3+} ion is surrounded by an almost octahedral arrangement of halide ions, and it is this local symmetry rather than the translational symmetry which dominates the optical properties from 1 to at least 6-7 eV. Several sharp reflectivity peaks have been found in this region which are believed to be due to parity-allowed molecular orbital transitions of the charge-transfer type. For $CrBr_3$ a peak occurs at 3.75 eV which agrees well with the value predicted by extrapolation of Kerr rotation data taken at lower energies.[1] The spectrum of CrI_3 is very similar to that of $CrBr_3$ with all the structure shifted to longer wavelengths. In the interpretation of the results the relevancy of the molecular orbital and energy band theories to different parts of the spectrum will be discussed.

---

[1] W. Jung, J. Appl. Phys. 36, 2422 (1965).

SERIES II VOLUME 13 NUMBER 3 ■ PUBLISHED FOR THE AMERICAN PHYSICAL SOCIETY BY THE AMERICAN INSTITUTE OF PHYSICS ● MARCH 1968 ■ PAGES 347–542

bulletin
OF THE AMERICAN PHYSICAL SOCIETY

INCLUDING THE PROGRAM OF THE
1968 MARCH MEETING IN BERKELEY
18-21 MARCH 1968

optical path length of about 10 mm. An analysis of the relative intensities of the Zeeman components was performed on an IBM 7094 using the theory given by Ofelt[1] and Judd.[2] It was assumed that the magnetic field is dominate in the ^8S ground state and weak in comparison with the crystal field in the excited state. The calculations are described and compared to experiment.

---

*This work, in part, was performed at and supported by the U. S. Air Force Materials Laboratory, W-PAFB.

[1] G. S. Ofelt, J. Chem. Phys. 37, 511 (1962).

[2] B. R. Judd, Phys. Rev. 127, 750 (1962).

CK6. Luminescence in MgO.* W. A. SIBLEY, C. M. NELSON,† and Y. CHEN, *Solid State Division, Oak Ridge National Laboratory*.—The phosphorescence and x-ray stimulated luminescence of a series of nominally pure MgO crystals have been investigated. Our results are in agreement with the assignment, by earlier workers, of the 1.7- and 2.5-eV luminescence bands to Cr^{3+} and Ni^{2+}, respectively. We tentatively assign the 1.4-eV emission band to $Mg(OH)_2$ impurity and discuss the effect of electron and neutron irradiation on the luminescence properties of these crystals.

---

*Research sponsored by the U. S. Atomic Energy Commission under contract with Union Carbide Corporation.

†Present address: Emory and Henry College, Emory, Va.

CK7. Charge-Transfer Spectra of Transition Metal Ions in Corundum. H. H. TIPPINS, *Aerospace Corporation*.—The ultraviolet absorption spectrum of corundum (Al_2O_3) containing dilute concentrations of the 3*d* series transition metal ions Ti^{3+}, V^{3+}, Cr^{3+}, Mn^{4+}, Fe^{3+} and Ni^{3+} was measured at room temperature and liquid-nitrogen temperature for photon energies in the range 3–9 eV. The most important features of the observed spectra are: (1) The peak positions are characteristic of the particular impurity ion, (2) The peak positions and widths (~0.5 eV) are independent of temperature over the range studied, and (3) The integrated intensities are strong. The spectra are identified with the allowed transition whereby an electron is transferred from a nonbonding orbital, localized predominantly on the $O^=$ ligands, to either the $t_{2g}(\pi^*)$ or $e_g(\sigma^*)$ antibonding orbital localized predominantly on the metal ion. The ions V^{3+}, Cr^{3+}, and Fe^{3+} show a correlation between the 3rd ionization potential and the position of the lowest energy absorption peak which is in good agreement with the charge transfer model. Lack of correlation for the remaining ions is attributed to the different valence state of Mn^{4+} and the possibility that more than 1 valence state is present in the Ti^{3+} and Ni^{3+} samples.

CK8. Stress Effects on Some Optical Excitations in CoF_2.* R. M. MacFARLANE (introduced by A. L. Schawlow) and J. W. ALLEN, *Stanford University*.—We have studied the effect of uniaxial stress on several optical absorption lines associated with the $(t_2^5e^2)^4T_1 \rightarrow (t_2^3e^4)^4A_2$ transition in piezomagnetic CoF_2. Data will be presented on the splittings and shifts of these lines for stress parallel to the (001) and (110) directions. It is found that the lowest energy σ polarized $(\Gamma_1^+ + \Gamma_2^+)$ exciton splits under stress with a coefficient of 0.2 $cm^{-1}/kg \cdot mm^{-2}$. This shows that the Davydov splitting of this level is $<0.5\ cm^{-1}$, indicating that the off-diagonal exchange between Co ions on different sublattices is very small. Such is also the case in MnF_2.[1] The split components show a small intensity variation with stress.

---

*Work supported in part by the U. S. Army Research Office (Durham) and in part by the National Science Foundation.

[1] R. E. Dietz, A. Misetich, and H. J. Guggenheim, Phys. Rev. Letters 16, 841 (1966).

CK9. Optical Properties of Chromium Trihalides in the Region 1–11 eV. PAUL M. GRANT and G. BRYAN STREET, *IBM Research Laboratory, San Jose*.—The normal incidence optical reflectivity of thin single crystal platelets of $CrBr_3$ and CrI_3 has been measured over the range 1–11 eV. $CrBr_3$ is hexagonal with the *c* axis normal to the platelet surface; CrI_3 is believed to have the same structure. Each Cr^{3+} ion is surrounded by an almost octahedral arrangement of halide ions, and it is this local symmetry rather than the translational symmetry which dominates the optical properties from 1 to at least 6–7 eV. Several sharp reflectivity peaks have been found in this region which are believed to be due to parity-allowed molecular orbital transitions of the charge-transfer type. For $CrBr_3$ a peak occurs at 3.75 eV which agrees well with the value predicted by extrapolation of Kerr rotation data taken at lower energies.[1] The spectrum of CrI_3 is very similar to that of $CrBr_3$ with all the structure shifted to longer wavelengths. In the interpretation of the results the relevancy of the molecular orbital and energy band theories to different parts of the spectrum will be discussed.

---

[1] W. Jung, J. Appl. Phys. 36, 2422 (1965).

CK10. Bimolecular Quenching of Mn^{++} Fluorescence in Calcium Fluorophosphate Single Crystals. JOSEPH MURPHY and F. M. RYAN, *Westinghouse Research Laboratories, Pittsburgh*.—The flash excitation luminescence decay characteristics of Mn^{2+} were studied in calcium fluorophosphate single crystals. The crystals, containing up to 1% Mn^{2+}, were pumped with short excitation pulses of variable intensity with a zenon flash tube and with an electron beam. Analysis of the decay was performed over 2 decades of intensity using a multichannel storage analyzer. Under low levels of excitation the Mn^{2+} luminescence was found to decay exponentially with a decay time of 8 msec. Under high levels of electron beam excitation the Mn^{2+} luminescence was found to follow a hyperbolic decay law for early times ($\ll$8 msec) which became exponential for late times ($\gg$ 8 msec). The ratio of percent hyperbolic decay to exponential increased with both the pumping intensity and the Mn^{2+} concentration. These results are explained by the theory of Tolstoi and Abramov[1] in which 2 interacting Mn^{2+} ions, both in the excited state for fluoresence can give rise to a nonradiative quenching process in which 1 Mn^{2+} reverts to its ground state without emitting a photon. Its energy is absorbed in raising the electron on the other Mn^{2+} to a higher excited state.

---

[1] N. A. Tolstoi and A. P. Abramov, Opt. Spectry. 20, 273 (1966).

CK11. Exchange Interactions in Excited States of Chromium Pairs in Ruby. M. H. L. PRYCE, *University of Southern California*.—Exchange interactions in excited states take on a more complicated form than the $JS \cdot S'$ applicable to the ground state. Because the electrons occupy the same orbitals in the ^2E and $^4A_2$ states, in the octahedral approximation, one can represent the exchange interaction for these states by a sum over electron pairs on different ions, of terms $J_{ab}\, S_a \cdot S_b$. Taking into account the C_3 distortion and spin-orbit interactions, the resulting excited states can be classified by the component of total spin along the *c* axis, and by symmetry with respect to ion interchange. Calculation of the energies reduces to diagonalizing 4 × 4 matrices. There are rigid selection rules for optical transitions. For nearest neighbors, 2 exchange parameters enter into the energy, but for less symmetrically related pairs, up to 9 parameters may be required.

I. Introduction

In recent years, much work has been done and much knowledge gained using the technique of normal incidence reflectivity to study very strong optical absorptions in covalent semiconductors and metals. Band theory, using the concept of interband critical point transitions, has been quite successful in classifying the observed phenomena.

We believe that reflectivity can also be useful for studying other kinds of strongly absorbing systems whose electronic structure may not be best formulated in terms of an itinerant electron theory. Such systems exist in certain magnetic insulators, of which chromium trihalides are an example, where the electronic structure seems better described by a localized molecular orbital theory. Another way of saying this is that the microsymmetry surrounding each cation is more important in classifying the electronic states than the space group of the unit cell.

II. Chemistry (Slide of Unit Cell)

This slide shows the unit cell of $CrBr_3$, CrI_3, and also $CrCl_3$ for its phase below 240°K. Note the layered structure of the unit cell and that each Cr^{3+} is surrounded by six halides in an octohedral symmetry with slight trigonal distortion. It is this microsymmetry we employ in discussing our optical results.

The crystals were grown by vapour growth methods in the shape of small, flat, single crystal platelets with the surface normal to the c-axis. Our reflectivity measurements were made off of this face. Chromium trihalides decompose in ambient atmosphere, hence all optical measurements were taken in vacua.

III. Reflectivity Curves for $CrBr_3$, CrI_3 (2 slides, 300, 85°K)

This slide shows the room temperature normal incidence reflectivity of $CrBr_3$ and CrI_3 from 1-11 eV. The curve for CrI_3 is displaced upwards from that of $CrBr_3$ for clarity. Incidentally, these spectra were taken with a computer controlled spectrophotometric system in which the computer set the wavelength, read and reduced the data. This relieved much of the tedium involved in taking and dividing scans and allowed repetition and averaging of runs to confirm the presence of the weaker structure.

Beginning in the near infrared for $CrBr_3$, we have multiple interference fringes due to the thinness of the sample. As the first crystal field transition sets in, the reflectivity drops as we no longer see the back side of the sample in addition to the front. A small bump indicates the presence of the $^4T_2$ Laporte-forbidden crystal field d-d transition. Between this and the next d-d transition another window opens up to the back side of the sample until the $^4T_1$ transition is reached, as indicated by the small bump here. Thereafter quite strong transitions begin and last throughout the visible and vacuum UV. Note that the structure for CrI_3 corresponds to that of $CrBr_3$ except that it is almost rigidly shifted about 1.2 eV to lower energies.
In passing, we point out that we believe the two bumps on the side of first CrI_3 peak are the $^4T_2$ and $^4T_1$ crystal field transitions in this material.

Dillon, Kamimura, and Remeika have measured absorbtion and magneto-optic spectra in Chromium trihalides; for $CrBr_3$ in particular covering the range 1.5 - 2.7 eV. Jung continued the measurements, using ellipsometry, over the first peak to about 3.5 eV. More about their interpretation later.

Although we performed Kramers-Kronig analyses, using four different extrapolation procedures, we believe the procedure of ~~filtering~~ fitting gaussian lines to the reflectivity data is more physically realistic. We believe this, firstly, because Jung found that with two gaussians he was able to obtain a very close fit to this peak here. The second gaussian inferred this second peak and we found it exactly where he predicted. Secondly, we have performed numerical experiments calculating reflectivity from gaussian line shapes and find qualitatively the structure shown here; particularly these bumps, and most of all these dips here arising from oscillations in the real part of the dielectric constant. These dips bothered us at first because they were quite different from anything we had seen in semiconductor spectra.

The next slide shows the same two materials near liquid N_2 temperature. The d-d transitions become narrower resulting in larger windows to the back side. There is a fair amount of sharpening of the reflectivity peaks, but very little shift. In fact, we think an upper limit for the magnitude of the shift of the two low energy peaks would be about 1×10^{-4} eV/K°. Measurements in the past of the temperature coefficient of the absorption toil of strong peaks like this have led to erroneously large values reported for the transition themselves. What was really being observed was line narrowing.

Recapitulating, the layered unit cell structure, the reflectivity peaks appearing to arise from gaussian dielectric constant lines, and the low temperature coefficients all argue strongly in these solids for a localized electronic structure to which we now turn our attention.

IV. MO Diagram for ML_6 Complex (1 Slide)

This slide shows schematically the molecular orbital energy levels for a general d-electron metal-ligand complex. The atomic orbitals involved are shown on the left for the cation and the right for the ligands. The dotted lines to the MO levels indicate non-vanishing two-centered overlap integrals. Parity forbidden transitions among states arising out of the t_{2g} and e_g orbitals are of course intensely studied by crystal field spectroscopists. We will be concerned with parity allowed transitions among all these levels.

V. Parity Allowed Transitions for CrX_3

Here we have displayed all the various parity allowed transitions for a chromium trihalide complex. The ground state is comprised of 3 t_{2g} electrons with all levels below completely filled. We have arbitrarily divided the transitions into 5 groups. At lowest energy are the well-known electron transfer transitions of π and σ type. Generally, the π-processes are weak compared to σ-processes as can be seen by comparing overlaps of the initial state atomic orbitals with the final state orbitals. Some hold that the π-processes are of the same strength as d-d transitions.

At somewhat higher energies we have the so-called interconfigurational transition which is analogous to the $3d^3 - 3d^2 4_p$ transition in the free ion. Note that it is quite strong.

Finally, we have at still higher energies transitions which I call IB_s and IB_p transitions (depending on the final state) because they are reminescent in their initial and final states of the interband transitions of semiconductors.

Before turning back to the data, let me remark that the transitions to the e_g level should appear at lower energies than those to t_{2g} from the same initial state. The reason is that by causing electron-transfer to these levels we are making Cr^{2+} and by Hund's rule the extra electron likes to go unpaired into e_g rather than paired into t_{2g}. For $CR^{3+} \rightarrow Cr^{2+}$, the energy difference should be of the order $6B + 5C - 10D_q$.

VI. Room Temperature Reflectivity Data (1 slide)

We will only have time to discuss assignments to the two major low energy peaks. Dillon and co-workers, on the basis of the circular dichroism of the absorption tail to the first edge assigned to the first peak to a σ-process and the second peak to the interconfiguration transition, arguing that the π-process would be too weak to be seen. We do not feel comfortable with these assignments with regard to our data and believe others might be possible.

The first question to raise is 'where are the π transitions?' Even if their strength is as small as the d-d transitions we feel we should see them because we do see the d-d's. Jung obtained an excellent fit with two gaussians with no discernible room left for extra structure near the first peak. In the low temperature reflectivity we see no extra structure in the first peak in $CrBr_3$.

The interconfigurational assignment for the second peak corresponds to the transition $3d^3 - 3d^2 4_s$ in the free ion with energy 18 eV. This means that in the solid this energy would have to be reduced to 3.75 eV in $CrBr_3$ and 2.65 eV in CrI_3, whereas a simple electrostatic model employing the dielectric constant would suggest energies in the range 7-9 eV. Furthermore, the almost rigid translation of this peak with respect to other structures in going from $CrBr_3$ to CrI_3 implies an inordinately large effect of the ligand σ, π orbitals on the position of the t_{1u} (σ*π*) orbital. On the other hand, we know that the ligand σ, π states, and the molecular orbitals derived therefrom, move closer to the t_{2g}, e_q levels with increasing ligand atomic number and this provides a simple explanation of the shifts of the peaks provided they arise from σ, π processes. In fact we would like to suggest that structure lying to the left of these big dips belongs to π and σ electron-transfer processes while that on the right belongs to interband and interconfigurational processes. In the absence of definitive energy level calculations for these solids, we feel unable to make positive assignments in detail at this time.

VII. Blow-Up of Two Low Energy Peaks (2 slides)

We mentioned previously that we saw no new structure, only narrowing, appearing in the first two reflectivity peaks of $CrBr_3$ and this slide illustrates this. However, in the next slide we see the case for CrI_3.

Note, however, that in addition to the $^4T_1$ d-d shoulder, we have two peaks appearing in the low temperature data. Since we do not observe this behavior in $CrBr_3$, we must ask what extra structure could appear in going from Br to I. It is well known that the spin-orbit splitting of the π orbitals is much larger for iodine than bromine. The splitting, of course, would have the largest chance of being observable for a π-process transition. The difference energy between the two peaks is 0.135 eV; DKR calculate the SO coupling constant for a π-process transition in CrI_3 to be .125 eV. Therefore, perhaps we can ascribe the first peak to the strongest π-process transition $t_{1u}(\pi^b) \rightarrow t_{2g}(\sigma^*)$ and the second peak to the strongest σ-process $t_{1u}(\sigma^b) \rightarrow e_g(\sigma^*)$. In passing we might mention that the final state for both σ and π processes is a John-Teller ion (Cr^{2+}) and it is remotely possible that the observed doublet is due to this effect.

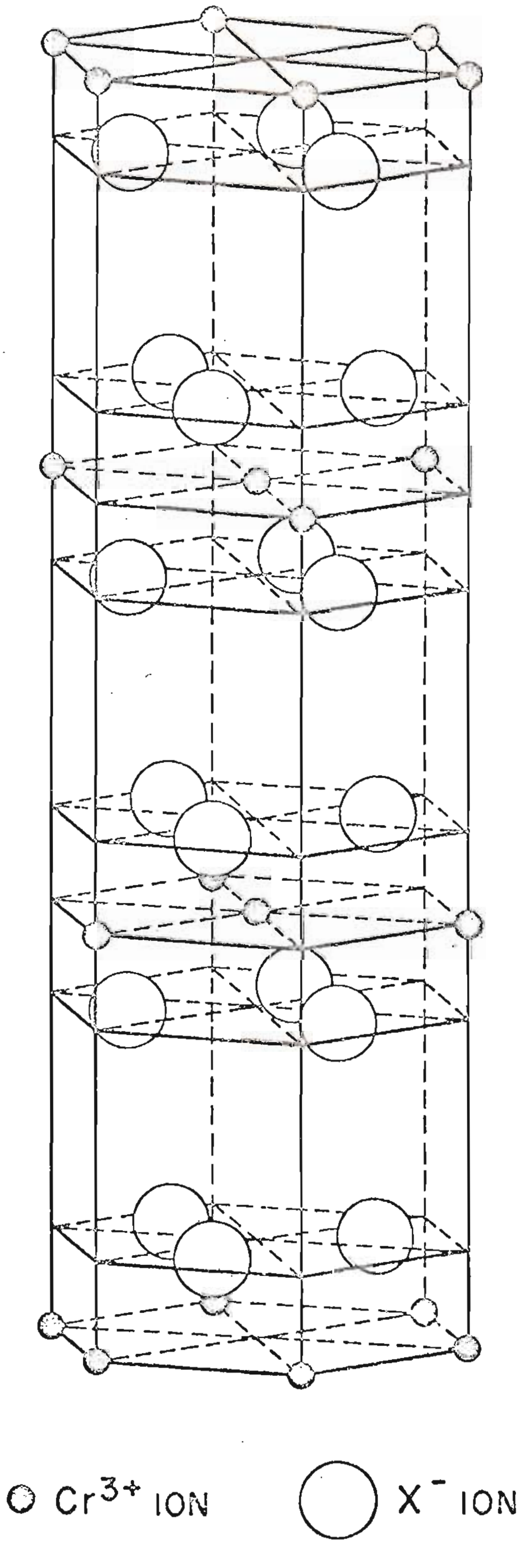

Cr X_3

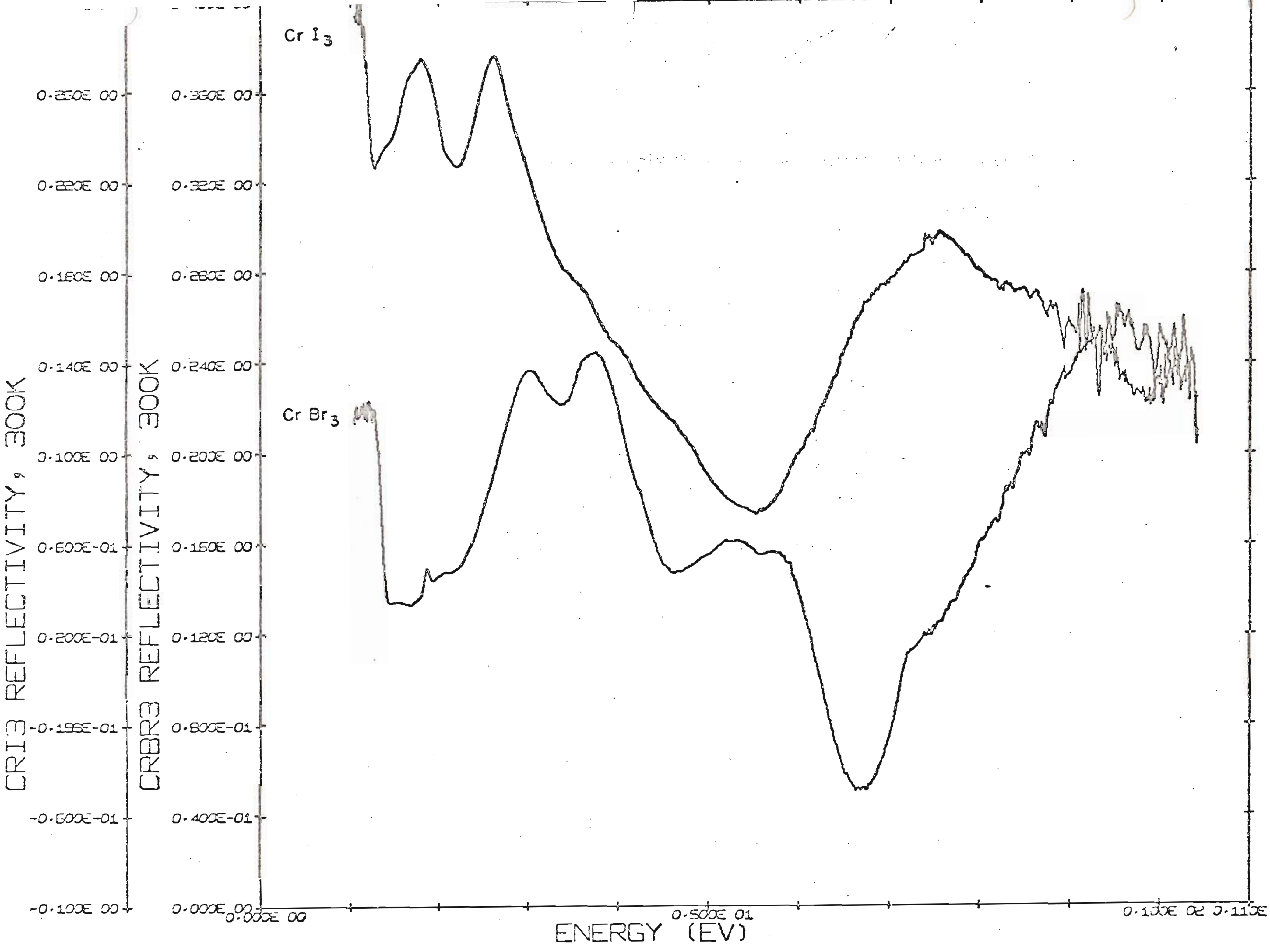
Cr I$_3$
Cr Br$_3$
CRI3 REFLECTIVITY, 300K
0.260E 00
0.220E 00
0.180E 00
0.140E 00
0.100E 00
0.600E-01
0.200E-01
-0.195E-01
-0.600E-01
-0.100E 00
CRBR3 REFLECTIVITY, 300K
0.360E 00
0.320E 00
0.280E 00
0.240E 00
0.200E 00
0.160E 00
0.120E 00
0.800E-01
0.400E-01
0.000E 00
0.000E 00
0.500E 01
0.100E 02
0.110E
ENERGY (EV)

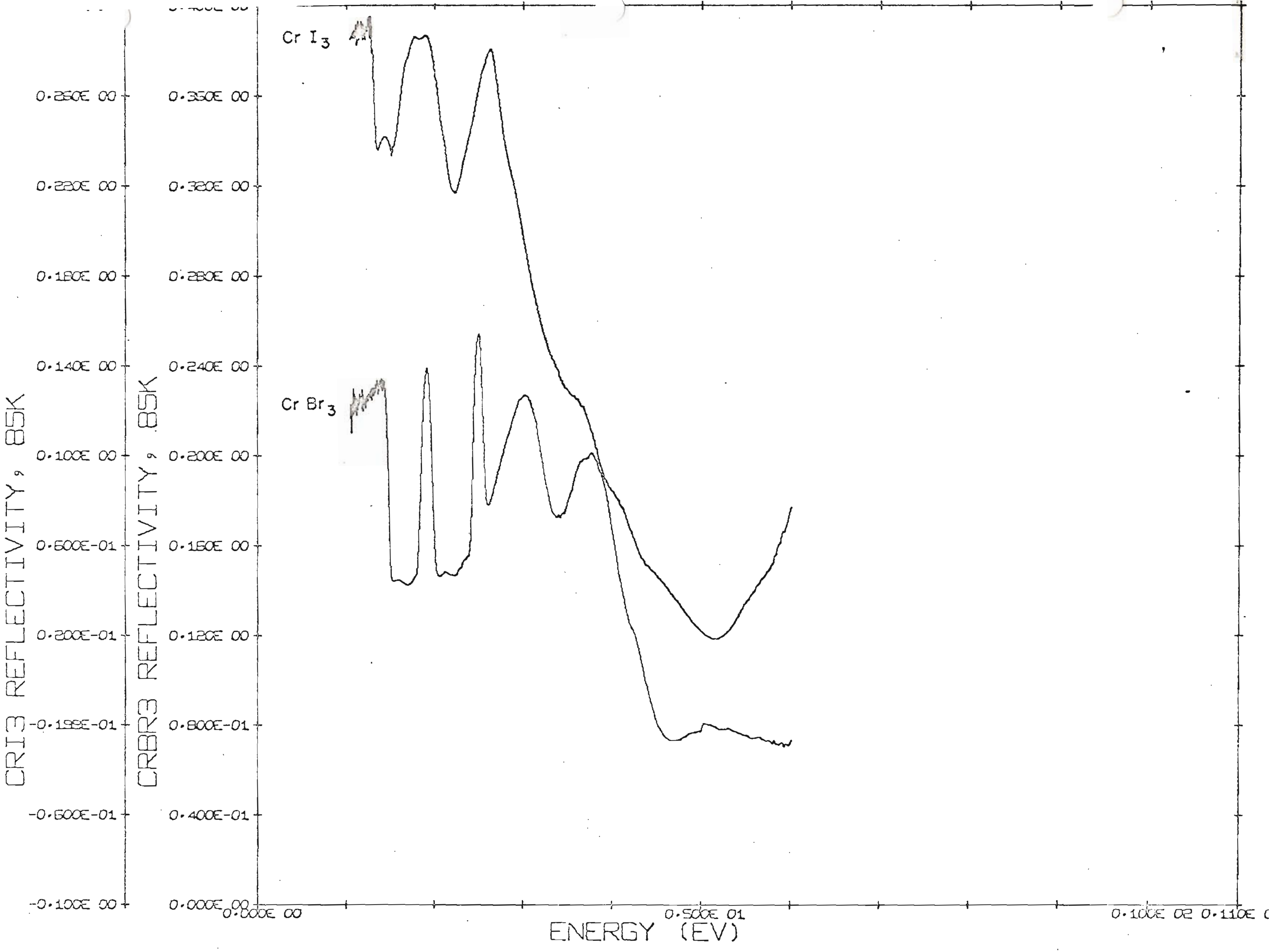
Cr I3
Cr Br3
CRI3 REFLECTIVITY, 85K
CRBR3 REFLECTIVITY, 85K
0.260E 00
0.220E 00
0.180E 00
0.140E 00
0.100E 00
0.600E-01
0.200E-01
-0.199E-01
-0.600E-01
-0.100E 00
0.360E 00
0.320E 00
0.280E 00
0.240E 00
0.200E 00
0.160E 00
0.120E 00
0.800E-01
0.400E-01
0.000E 00
0.000E 00
0.500E 01
0.100E 02
ENERGY (EV)

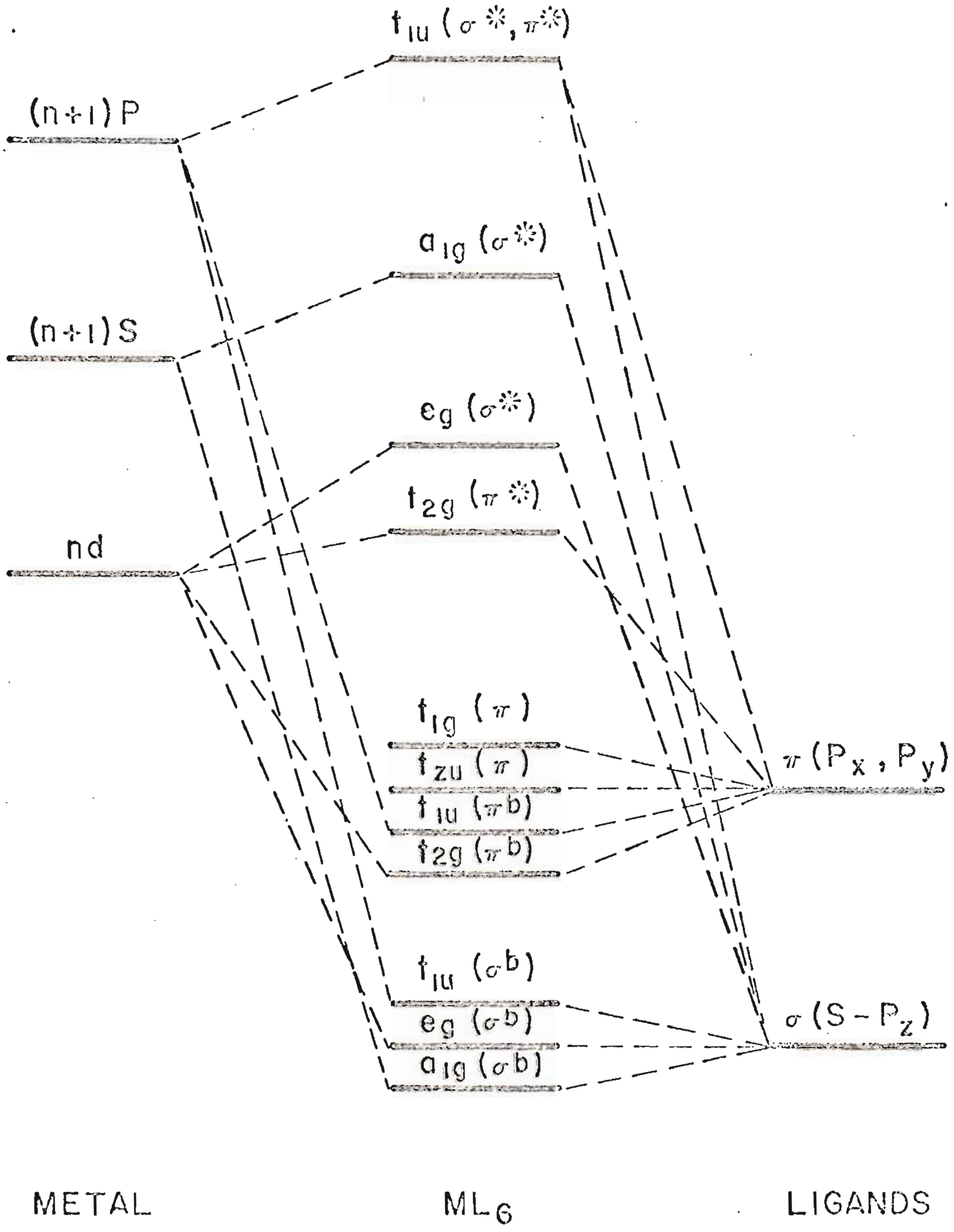

MOLECULAR-ORBITAL ENERGY-LEVEL DIAGRAM FOR AN OCTAHEDRAL METAL-LIGAND COMPLEX

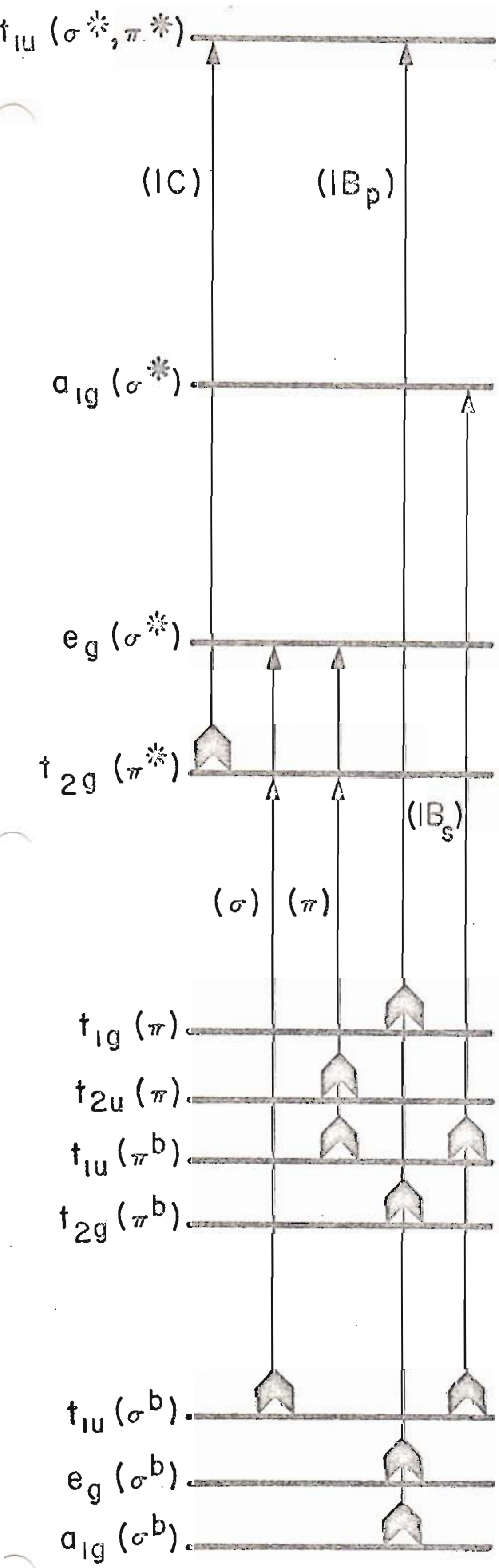

PARITY ALLOWED TRANSITIONS

	TRANSITION & TYPE	OVERLAP INTEGRAL	RELATIVE OSCILLATOR STRENGTH
IB_p	$a_{1g}(\sigma^b) \rightarrow t_{1u}(\sigma^*, \pi^*)$	$S(\sigma, P\sigma)$	
	$e_g(\sigma^b) \rightarrow t_{1u}(\sigma^*, \pi^*)$	$S(\sigma, P\sigma)$	
	$t_{2g}(\pi^b) \rightarrow t_{1u}(\sigma^*, \pi^*)$	$S(\pi, P\sigma)$	
	$t_{1g}(\pi) \rightarrow t_{1u}(\sigma^*, \pi^*)$	$S(\pi, P\sigma)$	
IB_s	$t_{1u}(\sigma^b) \rightarrow a_{1g}(\sigma^*)$	$S(\sigma, S)$	
	$t_{1u}(\pi^b) \rightarrow a_{1g}(\sigma^*)$	$S(P\sigma, S)$	
IC	$t_{2g}(\pi^*) \rightarrow t_{1u}(\sigma^*, \pi^*)$		10
σ	$t_{1u}(\sigma^b) \rightarrow t_{2g}(\pi^*)$	$S(\pi, d\pi)$	0.01
	$t_{1u}(\sigma^b) \rightarrow e_g(\sigma^*)$	$S(\sigma, d\sigma)$	1
π	$t_{1u}(\pi^b) \rightarrow t_{2g}(\pi^*)$	$S(P\pi, d\pi)$	0.1
	$t_{2u}(\pi) \rightarrow t_{2g}(\pi^*)$	$S(\pi, d\pi)$	
	$t_{1u}(\pi^b) \rightarrow e_g(\sigma^*)$	$S(P\sigma, d\sigma)$	0.01
	$t_{2u}(\pi) \rightarrow e_g(\sigma^*)$	$S(\pi, d\sigma)$	

PARITY ALLOWED TRANSITIONS
IN AN OCTAHEDRAL ML_6 COMPLEX

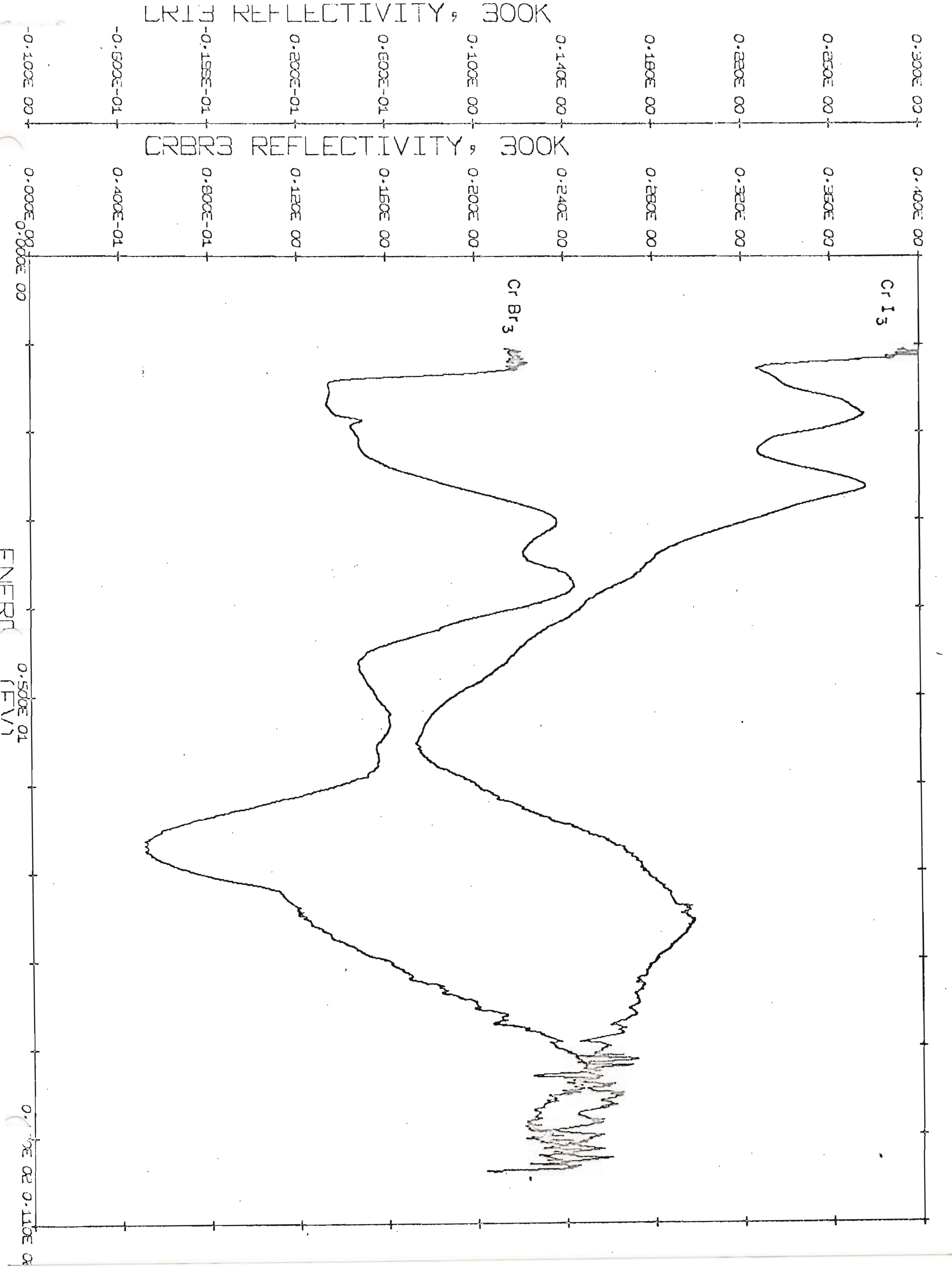

CRI3 REFLECTIVITY, 300K
-0.100E 00
-0.600E-01
-0.199E-01
0.200E-01
0.600E-01
0.100E 00
0.140E 00
0.180E 00
0.220E 00
0.260E 00
0.300E 00
CRBR3 REFLECTIVITY, 300K
0.000E 00
0.400E-01
0.800E-01
0.120E 00
0.160E 00
0.200E 00
0.240E 00
0.280E 00
0.320E 00
0.360E 00
0.400E 00
Cr Br$_3$
Cr I$_3$
0.000E 00
0.500E 01
0.110E 02
ENERG
(EV)

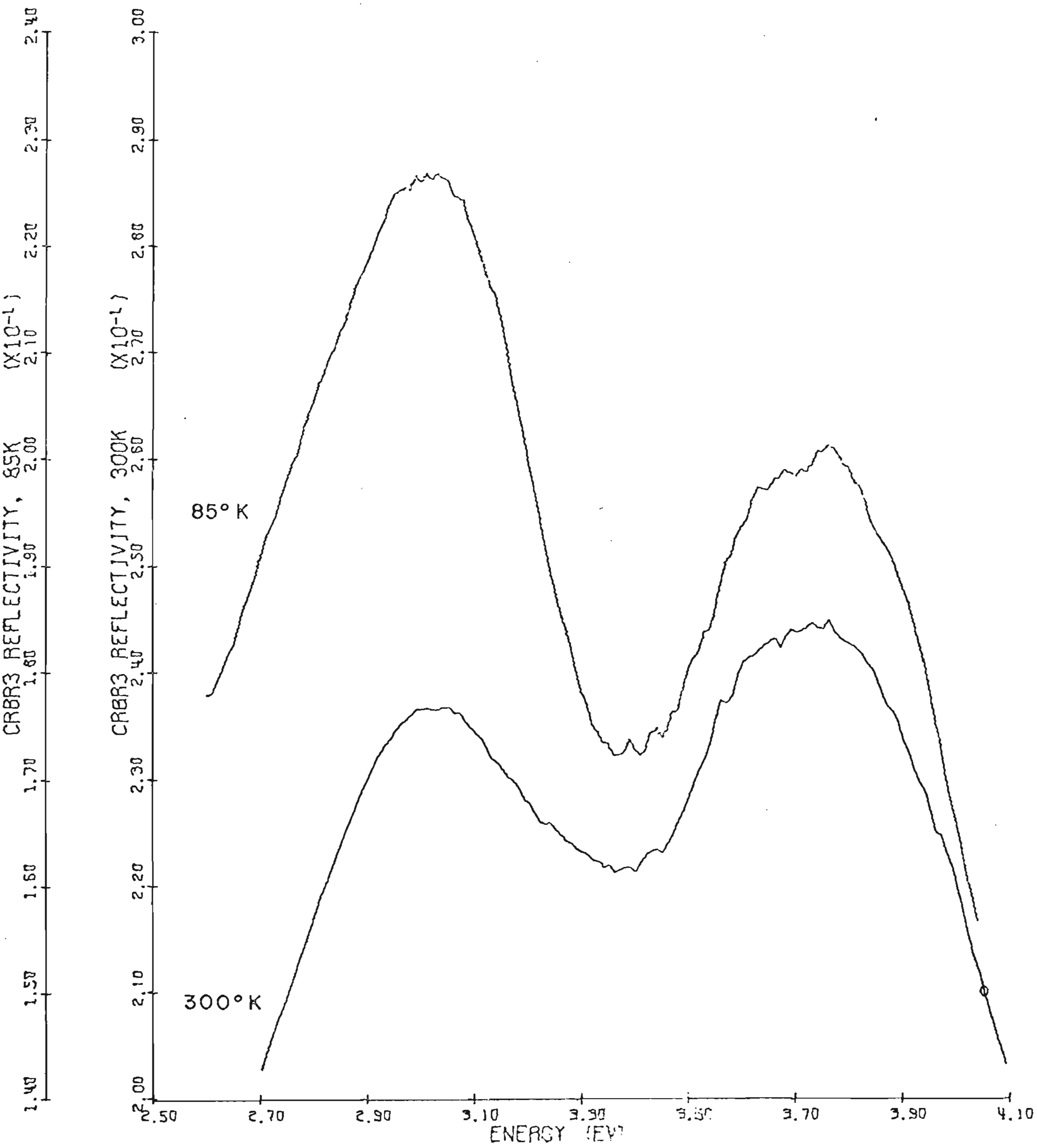
CRBR3 REFLECTIVITY, 85K (X10-1)
1.40
1.50
1.60
1.70
1.80
1.90
2.00
2.10
2.20
2.30
2.40
CRBR3 REFLECTIVITY, 300K (X10-1)
2.00
2.10
2.20
2.30
2.40
2.50
2.60
2.70
2.80
2.90
3.00
85° K
300° K
2.50
2.70
2.90
3.10
3.30
3.50
3.70
3.90
4.10
ENERGY (EV)

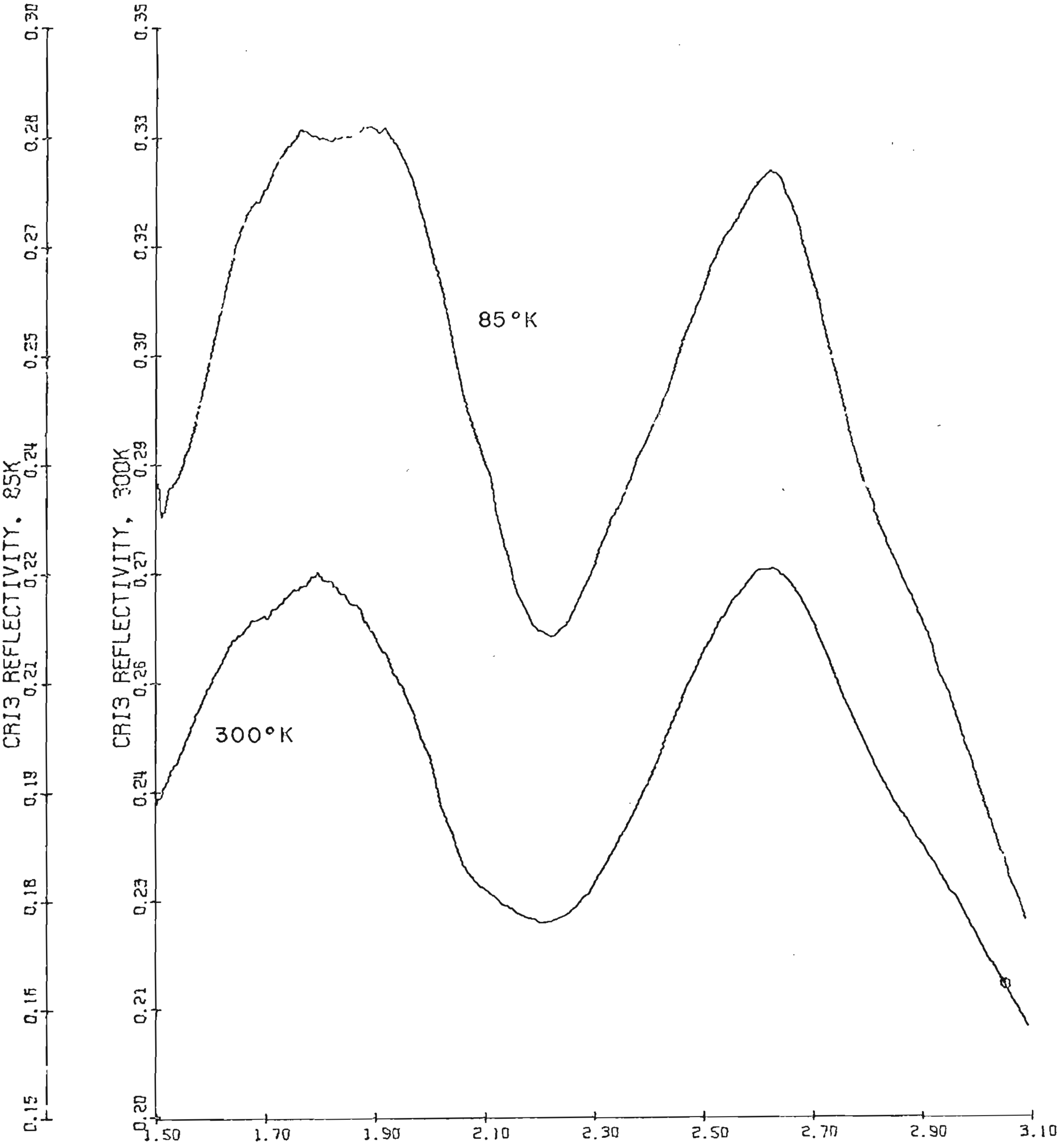
CRI3 REFLECTIVITY, 85K
0.15
0.16
0.18
0.19
0.21
0.22
0.24
0.25
0.27
0.28
0.30
CRI3 REFLECTIVITY, 300K
0.20
0.21
0.23
0.24
0.26
0.27
0.29
0.30
0.32
0.33
0.35
1.50
1.70
1.90
2.10
2.30
2.50
2.70
2.90
3.10
85°K
300°K